



<b>Publication Year</b>	2016
<b>Acceptance in OA @INAF</b>	2020-06-15T08:57:05Z
<b>Title</b>	Radio properties of Compact Steep Spectrum and GHz-Peaked Spectrum radio sources
<b>Authors</b>	ORIENTI, Monica
<b>DOI</b>	10.1002/asna.201512257
<b>Handle</b>	<a href="http://hdl.handle.net/20.500.12386/26049">http://hdl.handle.net/20.500.12386/26049</a>
<b>Journal</b>	ASTRONOMISCHE NACHRICHTEN
<b>Number</b>	337

# Radio properties of Compact Steep Spectrum and GHz-Peaked Spectrum radio sources

M. Orienti<sup>1,\*</sup>

INAF-IRA, Via Gobetti 101, 40129 Bologna, Italy

Received XXXX, accepted XXXX

Published online XXXX

**Key words** galaxies: active, radio continuum: general, radiation mechanism: non-thermal, polarization, radio lines: ISM

Compact steep spectrum (CSS) and GHz-peaked spectrum (GPS) radio sources represent a large fraction of the extragalactic objects in flux density-limited samples. They are compact, powerful radio sources whose synchrotron peak frequency ranges between a few hundred MHz to several GHz. CSS and GPS radio sources are currently interpreted as objects in which the radio emission is in an early evolutionary stage. In this contribution I review the radio properties and the physical characteristics of this class of radio sources, and the interplay between their radio emission and the ambient medium of the host galaxy.

Copyright line will be provided by the publisher

## 1 Introduction

Compact steep spectrum (CSS) and GHz-peaked spectrum (GPS) radio sources are powerful ( $P_{1.4\text{ GHz}} > 10^{25}\text{ W/Hz}$ ) and compact objects with angular sizes not exceeding 1 – 2 arcsec. The main peculiarity of these objects is the convex synchrotron radio spectrum that peaks around 100 MHz in the case of CSS sources, and at about 1 GHz in the case of GPS objects, or even up to a few GHz in the sub-population of high frequency peakers (HFP) defined by Dallacasa et al. (2000). Above the peak frequency the spectrum is steep with a spectral index  $\alpha \sim 0.7$  ( $S_\nu \propto \nu^{-\alpha}$ ).

Depending on both the frequency and the flux-density limit of the catalogues used, the CSS/GPS samples are dominated by different sub-classes of objects. Bright CSS and GPS samples have been selected from the 3C, PW and 1-Jansky catalogues (see, e.g., Spencer et al. 1989, Fanti et al. 1990, Stanghellini et al. 1998). On the other hand, deep catalogues, like B3, FIRST, WENSS and AT20GH, were used for selecting weak samples (e.g., Fanti et al. 2001, Snellen et al. 1998, Kunert et al. 2002, Hancock et al. 2010). In the last decades other samples of CSS/GPS candidates were constructed using different selections tools like the radio morphology, optical counterpart, compact linear sizes (e.g., COINS sample, Peck & Taylor 2000; CSS-VIPS sample, Tremblay et al. 2009; CORALZ, Snellen et al. 2004), as well as polarization properties (Cassaro, Dallacasa & Stanghellini 2009).

Statistical analysis of CSS/GPS samples pointed out an empirical anti-correlation between the peak frequency of the spectrum and the linear size (O’Dea & Baum 1997). This has been interpreted either in terms of synchrotron-self absorption related to the compact dimension of the sources

(e.g., Snellen et al. 2000, Fanti 2009, Orienti & Dallacasa 2008a) or due to free-free absorption from an ionized medium enshrouding the radio emission (e.g., Bicknell et al. 1997, Tingay et al. 2015, Callingham et al. 2015), although a combination of both mechanisms may take place (e.g., Orienti & Dallacasa 2008a).

CSS and GPS radio sources represent a significant fraction (15% – 30% depending on the frequency) of the sources in flux-density limited catalogues, opening a debate about their nature. Fanti et al. (1990) investigated whether the compact size is a result of projection effects, but they concluded that this was unlikely, leaving room only for a minority (<25%) of large objects foreshortened by geometrical effects. The intrinsically compact size of CSS/GPS is interpreted mainly in terms of *Youth*: these sources are small because they are still in an early stage of their evolutionary path, and may become/develop into Fanaroff-Riley type-I/II (FRI/FRII, Fanaroff & Riley 1974) radio sources (e.g., Fanti et al. 1995, Snellen et al. 2000, Alexander 2000, Perucho 2015). Strong supports to the *Youth Scenario* came from the estimate of the kinematic age by the determination of the hot spot separation velocity in a handful of the most compact objects (Polatidis 2009, Giroletti & Polatidis 2009, and references therein, Polatidis & Conway 2003, and references therein), as well as from the radiative age (Murgia 2003, Murgia et al. 1999, Nagai et al. 2006). The alternative scenario that postulated the presence of an exceptionally dense medium able to frustrate the jet growth was not supported by multi-band observations which pointed out that the gas of their host galaxies are similar to those of extended FRII sources (e.g., Fanti et al. 1995, Fanti et al. 2000, Siemiginowska et al. 2005).

In the next Sections I will briefly review the observational and physical properties of CSS and GPS radio sources.

\* Corresponding author: e-mail: orienti@ira.inaf.it

Radio properties are presented in Sections 2. In Section 3 I describe the physical parameters, such as the luminosity and the magnetic field, and how they evolve. In Section 4 I discuss the duty cycle of the radio emission, while in Section 5 and 6 I present the characteristics of the ambient medium and their role in producing the observed source asymmetries. A brief Summary is presented in Section 7.

Throughout the paper I assume  $H_0 = 71 \text{ km s}^{-1} \text{ Mpc}^{-1}$ ,  $\Omega_M = 0.27$ ,  $\Omega_\Lambda = 0.73$  in a flat Universe. The spectral index is defined as  $S_\nu \propto \nu^{-\alpha}$ .

## 2 Radio properties

### 2.1 Morphology

Due to their compact size, CSS/GPS sources appeared unresolved in single-dish observations, and only the advent of interferometers with sub-arcsecond resolution could pinpoint their radio morphology. CSS and GPS are divided into three main morphological classes: 1) symmetric (i.e. two-sided) structures; 2) core-jet structures; 3) complex morphology.

Symmetric objects have a two-sided radio structure resembling a scaled-down FR II radio source (Fig. 1). The main ingredients are mini-lobes and hot spots. Sometimes, a weak component hosting the core is present, and, depending on their size, CSS/GPS may be termed as “compact symmetric objects” (CSO) if they are smaller than 1 kpc, or “medium-sized symmetric objects” (MSO) if they extend up to 10 – 15 kpc (Fanti et al. 2001). However, a large fraction of “symmetric” sources have a very asymmetric two-sided morphology, where one side of the source is much brighter than the other (e.g. Saikia et al. 2003, Rossetti et al. 2006). When the core is detected it is usual to find that the brighter lobe is the one closer to the core. This is opposite to what is expected in presence of geometrical effects, suggesting some interaction between the jet and the ambient medium (see Section 6).

In two-sided objects the core usually represent a very small fraction (a few per cent) of the total radio emission of the source indicating the absence of beaming effects (e.g. Wilkinson et al. 1994). On the contrary, in radio sources with a core-jet and complex structure the core dominates the radio emission, suggesting the presence of significant boosting effects. In addition core-jet structures are usually found in CSS/GPS which are optically identified with quasars (e.g., Rossetti et al. 2004, Orienti et al. 2006), supporting the role of projection effects.

As in the case of core-jet structures, also complex morphologies are usually caused by boosting effects, at least in high-luminosity sample. This does not seem to hold in low-luminosity samples where a high fraction of sources ( $\sim 30\%$ ) have weak extended emission and distorted structures which are likely intrinsic (Kunert-Bajraszewska et al. 2010).

### 2.2 Variability

The spectral behaviour and the flux density variability is investigated by multifrequency observations, closely simultaneous when possible, carried out at various epochs. In past works CSS/GPS objects were considered the least variable extragalactic radio sources (O’Dea 1998). However, long-term monitoring campaigns found different results depending on the different sub-classes considered (CSS, GPS, HFP, quasars, galaxies). It turned out that many GPS/HFP sources are picked up with a convex spectrum only during flaring events, when the radio emission is dominated by the jet, while in their average state they possess a flat spectrum (Torniainen et al. 2005, Tinti et al. 2007). In particular, high fraction of CSS radio galaxies are not variable, while only  $\sim 30\%$  of GPS/HFP galaxies preserve the convex spectrum (Torniainen et al. 2007, Orienti et al. 2010, Hancock et al. 2010). The majority of the CSS, GPS, and HFP quasars show significant flux density and spectral variability (Mingaliev et al. 2012, Orienti et al. 2007).

Spectral changing and flux density variability do not always imply that the source is part of the blazar population, rather than a genuine CSS/GPS/HFP object. In fact, changes in the radio spectrum may be a direct consequence of the source expansion (e.g., Tingay & de Kool 2003). In newly born radio sources, the evolution time-scales can be of the order of a few tens of years. Changes in the radio spectrum of such young objects can be appreciable after the short time (5 – 10 yr) elapsing between the observing epoch. If the variability is due to the source expansion we expect that the peak shifts to lower frequencies, the flux density in the optically-thin regime decreases, while that in the optically-thick part of the spectrum increases. This behaviour has been observed in the HFP RXJ1459+3337 (Orienti & Dallacasa 2008b), as well as in a handful of HFP/GPS sources (Dallacasa & Orienti 2015, Orienti et al. 2010), although some additional variations in the free-free optical depth may be present (e.g., the GPS PKS 1718-649, Tingay et al. 2015).

### 2.3 Polarization

CSS/GPS objects are weakly polarized. Multifrequency polarimetric measurements of a sample of CSS/GPS radio sources (Fanti et al. 2004, Cotton et al. 2003) show that very compact objects ( $< 1 \text{ kpc}$ ) are unpolarized or strongly depolarized, and the fractional polarization is strictly related to the frequency: the lower the frequency, the stronger the depolarization. Furthermore, the fractional polarization does not increase gradually with the source size, but there seems to be a discontinuity at a “critical size” (the so-called *Cotton effect*), that is about 6 kpc at 1.4 GHz and moves down to about 1 kpc at higher frequencies.

The strong depolarization of the most compact objects may be related to the interstellar medium of the narrow line region (NLR) which acts as a Faraday Screen, depolarizing and/or rotating the polarized signal. The “amount” of de-

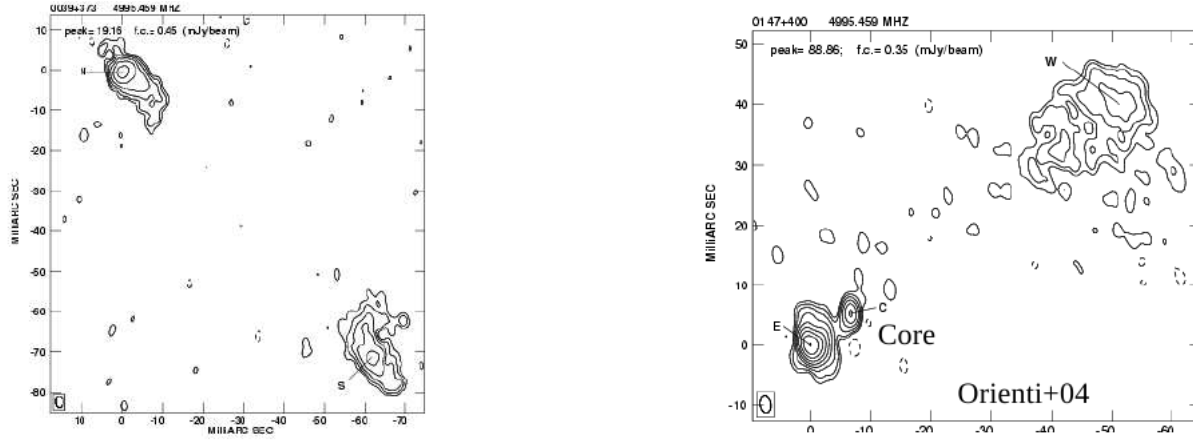


**Fig. 1** Examples of a symmetric “two-sided” CSO (left), and of an asymmetric one (right). Adapted from Orienti et al. 2004

polarization and/or rotation depends on both the inhomogeneities of the ambient medium and the distribution of the magnetic field. Support to the presence of a dense and inhomogeneous medium in front of the radio source comes from the large rotation measure (RM) estimated for those sources with some polarized emission. RM of the order of  $1000 \text{ rad m}^{-2}$  or even higher are commonly observed (e.g., O’Dea 1998, Cotton et al. 2006, Rossetti et al. 2008, Mantovani et al. 2013).

A different result was found by Mantovani et al. (2009) who studied a complete sample of CSS with multifrequency single-dish observations. In this case no drop in the polarization was found for the most compact sources. However, this apparent contradiction is likely due to the contamination by geometrically-foreshortened quasars. In fact, if the galaxies are considered separately, the *Cotton effect* is visible again, while the fractional polarization in quasars seems independent from the linear size. In addition, quasars have higher fractional polarization than galaxies, while galaxies experience larger RM. In HFP quasars the high fractional polarization is associated with low RM and high flux density variability (Orienti & Dallacasa 2008c), similar to what is found in blazars (Mantovani, Bondi, & Mack 2011). Sub-arcsecond resolution observations point out higher RM than those estimated by low-resolution single-dish observations suggesting the presence of blended components.

Another intriguing aspects pointed out by multifrequency observations is an increase of the polarized emission at low frequency (re-polarization). This may be explained either in terms of multiple unresolved components with different spectral characteristics that dominate at different frequencies, or in presence of variability (Mantovani et al. 2009, Orienti & Dallacasa 2008c). In this case the RM does not follow the  $\lambda^2$  correlation (see e.g., Burns 1966).

A remarkable result found is that CSS are more asymmetric in the polarization of the outer lobes than the extended galaxies (Saikia & Gupta 2003). The high incidence of po-

larization and morphological asymmetries observed in CSS and GPS is likely an indication of jet-gas interaction which is more probable when the radio jet is still piercing its way through the dense medium of the host galaxy (see Section 6).

### 3 Physical properties

In a scenario where radio sources grow in a self-similar way, the evolution of each radio object originated by an AGN depends on its linear size. The determination of the physical properties in objects at the beginning of their evolution is crucial for setting tight constraints on the initial conditions of the radio emission.

The source size, flux density, and the peak frequency are parameters that can be easily derived from the observations and then used as a starting point to determine the physical properties of the sources.

The existence of a relation between the rest-frame peak frequency and the projected linear size (e.g. O’Dea & Baum 1997) indicates that the mechanism responsible for the curvature of the spectrum is related to the source dimension, and thus to the source age. Interestingly, some of the most compact and asymmetric sources seem to depart from this relation. However, this is likely due to the presence of several sub-components that are responsible for different part of the total radio spectrum: one bright and compact hot spot dominates the radio emission, overwhelming the contribution from the extended structures (e.g. J1335+5844, Orienti & Dallacasa 2014).

Another important relationship to investigate is between the peak flux density and the peak frequency, since they provide constraints on the magnetic field in case the spectral curvature is due to SSA. The analysis of the peak flux density as a function of the peak frequency in CSS/GPS/HFP sources from bright samples suggests a segregation between sources

identified with galaxies and quasars. When only galaxies are considered there seems to be an anticorrelation between the peak flux density and the peak frequency, as expected if the spectral turnover is due to SSA, although FFA cannot be completely discarded. On the contrary, this anticorrelation does not hold in case of quasars. They have peak frequency in GHz regime, while the peak flux density covers three order of magnitudes, independently of the peak frequency, suggesting a different nature for the majority of galaxies and quasars (Orienti et al. 2010).

### 3.1 Magnetic field

The direct measurement of the magnetic field in extragalactic radio sources is a difficult task to carry out. An indirect way to estimate the magnetic field is to assume that the radio source is in minimum energy condition corresponding to a near equipartition of energy between the radiating particles and the magnetic field (Pacholczyk 1970). Although this condition is assumed in many evolutionary models, there is no a priori reason for believing that magnetic fields in radio sources are in equipartition.

As mentioned earlier, a direct measurement of the magnetic field from observable quantities is obtained by means of the spectral parameters. If the spectral peak is produced by SSA, we can compute the magnetic field  $H$  by using observable quantities only:

$$H \sim f(\alpha)^{-5} \theta^4 S_p^{-2} \nu_p^5 (1+z)^{-1} \quad (1)$$

where  $\theta$  is the source solid angle,  $\nu_p$  and  $S_p$  are the peak frequency and peak flux density, respectively,  $z$  is the redshift, and  $f(\alpha)$  is a function that depends weakly on the spectral index (Kellermann & Pauliny-Toth 1981). Scott & Readhead (1977) and Readhead (1994) computed the magnetic field for sources of low-frequency spectral turnovers close in value to the observing frequency and found that the magnetic fields inferred directly from the spectrum were within a factor of 16 of the equipartition values. However, there are no systematic studies of sources with spectra peaking at higher frequencies, i.e. objects younger than those in Scott & Readhead (1977).

The main difficulty in applying this method has been the uncertainty in determining source component parameters at the turnover frequency, which results in a limited accuracy of the magnetic field estimates. However this method may be used for GPS/HFP sources. The peak frequency around a few GHz gives the possibility to sample both the optically-thick and -thin part of the spectrum by multifrequency high resolution VLBA observations, leading to a fairly accurate estimate of the peak parameters.

The peak magnetic fields estimated for the components of HFP radio sources turned out to be in good agreement with those derived by assuming minimum energy conditions, supporting the idea that in general young radio sources are in minimum energy conditions and their spectral turnover is caused by SSA (Orienti & Dallacasa 2008a, 2008b, 2014).

However, there are a few exceptions where the peak magnetic field is orders of magnitude higher than the equipartition value. The analysis of the optically-thick part of the spectrum turned out to be more inverted than the limit value for SSA ( $\alpha < -2.5$ ), indicating that the spectral peak is due to FFA. Therefore the magnetic field determined by the peak values is meaningless.

Depending on the size of the sources, the estimated magnetic fields range from a few 150 mG in the most compact components of HFP radio sources down to 0.1 mG in the lobes of CSS (Fanti et al. 2001, Dallacasa et al. 2002, Orienti et al. 2006). The anticorrelation between the magnetic field strength and the linear size is in agreement with what is expected in case the source is adiabatically expanding. However, when the single source components are considered, it emerges that the field intensities found in the various components of the same object can vary up to an order of magnitude (Orienti & Dallacasa 2012). Such differences may arise from asymmetries in the source propagation, for example when the two sides experience a different environment (see Section 5), indicating that simple self-similar evolution models may be not adequate to describe the radio source growth (e.g., Sutherland & Bicknell 2007).

### 3.2 Luminosity evolution

Several evolutionary models<sup>1</sup> (e.g. Fanti et al. 1995; Readhead et al. 1996; Snellen et al. 2000) were proposed to describe how the physical parameters (i.e. luminosity, linear size and velocity) evolve as the radio emission grows within the host galaxy. The majority of the proposed models predict an increase of the luminosity and a decrease of the jet advance speed when the radio emission is still embedded within the dense medium of the NLR. Then, as the radio emission emerges from the NLR the luminosity is expected to decrease, while the jet advance speed should not vary significantly. These predictions should be validated by statistical studies of samples of CSS/GPS/HFP spanning a large range of linear size.

O’Dea (1998) studied the radio luminosity at 5 GHz as a function of the projected linear size, but no correlation was found. This may be related to the similar radio power of the selected sources. To determine how the luminosity evolves as the source grows, Orienti & Dallacasa (2014) studied a sample of 51 *bona fide* young radio sources with an unambiguous detection of the core region, and spanning a wide range of linear size, from a few pc up to tens of kpc, for high-luminosity radio sources. To get rid of possible boosting/projection effects that may contaminate the estimate of the physical parameters, only objects optically associated with galaxies were considered when searching for empirical relations.

<sup>1</sup> The evolutionary models considered in this review try to explain how an individual radio source grows and evolves, without taking into account any cosmological implication.

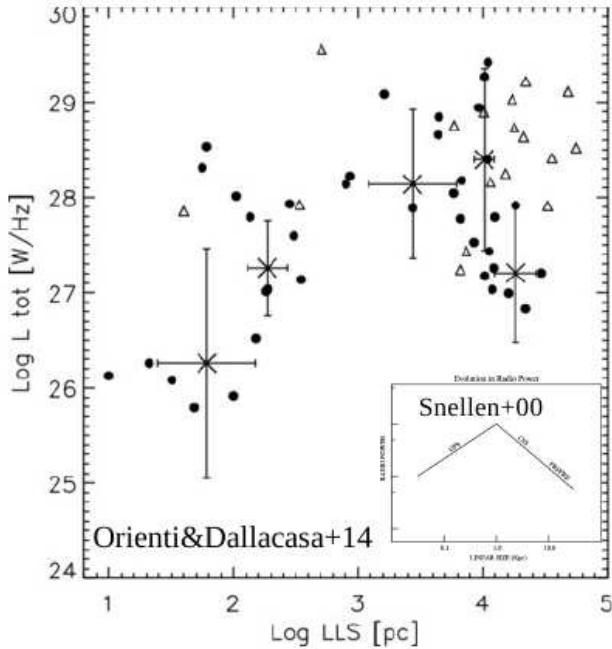


**Fig. 2** Total luminosity at 375 MHz versus the linear size for the sources of the sample selected by Orienti & Dallacasa (2014). Filled circles are galaxies, while empty triangles are quasars. Crosses represent the median values of the total luminosity and linear size, for galaxies only, separated into different bins. As a comparison, in the bottom right corner there is the evolutionary trend expected by the model developed in Snellen et al. (2000).

The analysis of the source luminosity at 375 MHz versus the linear size points out two different relations depending on the source size: sources smaller than a few kpc increase their luminosity as they grow, while larger sources progressively decrease their luminosity, in agreement with the evolutionary models (Fig. 2). The smallest sources reside within the innermost region of the host galaxy, where the dense and inhomogeneous ambient medium favours radiative losses. As the radio source expands on a kpc scale, it experiences a smoother and less dense ambient medium and adiabatic losses dominate.

Kunert-Bajraszewska et al. (2010) extended the analysis of the radio power as a function of linear size by including a sample of low-luminosity CSS objects having 1.4-GHz luminosity comparable to that of FRI. They found a clear distinction between high-power and low-power objects: the former seem to follow an evolutionary path similar to that expected by the models. The latter are located below this path and they may represent short-lived objects with a different fate.

## 4 The life-cycle of the radio emission

It is nowadays clear that powerful ( $L_{1.4 \text{ GHz}} > 10^{25} \text{ W/Hz}$ ) radio sources are a small fraction of the AGN generally associated with ellipticals, suggesting that the radio activity is a transient phase in the life of these systems. The typical age of active phase in radio sources is about  $10^7 - 10^8$  years, which is followed by a relic phase which is roughly one order of magnitude shorter (Parma et al. 2007).

The onset of radio emission is currently thought to be related to mergers which provide fuel to the central AGN. However, the reason why and when the radio emission switches off is still an open question. The excess of young objects in flux-limited samples suggests the existence of short-lived objects unable to become FR II, and additional ingredients, like the recurrence of the radio emission (e.g., Czerny et al. 2009), or the interplay between the source and the environment, must be considered (see Section 5). Support to the existence of short-lived objects come from statistical studies of the ages of CSO which peak at about 500 years (Gugliucci et al. 2005), and of the sub-class of low-luminosity CSS radio sources (Kunert-Bajraszewska et al. 2010).

If the supply of new relativistic particles turns off, the radio emission fades rapidly due to the severe energy losses and the radio spectrum steepens fast making these sources under-represented in flux-limited catalogues. Indeed, only a few objects have been suggested as faders so far, based on the absence of active regions (Kunert-Bajraszewska et al. 2005, 2006), and the distribution of spectral index found steep across the whole source, like in the case of PKS 1518+047 (Orienti, Murgia, & Dallacasa 2010).

A different situation is the recurrence of the radio emission in an AGN. In this case a “young” radio source, with new activity regions like the core and hot spots, is present close to the fossil of a previous epoch of the radio emission. A clear example of intermittent radio activity is the FR II radio galaxy B0925+420 where three different episodes of jet activity have been observed (Brocksopp et al. 2007).

Extended emission on the kpc-scale and beyond was discovered in the GPS galaxy J0111+3906 (Baum 1990), and interpreted in terms of the relic of a past radio activity which occurred about  $10^7$ - $10^8$  years ago. Recently, a remnant of about 160 kpc in size from an earlier stage of activity was found in the CSS galaxy B2 0258+35, suggesting that the time between subsequent phases of activity in this source is about  $10^8$  (Shulevski et al. 2012, Brienza et al. 2015).

Following the model by Czerny et al. (2009), the restarting of the radio emission may occur on much shorter (a few thousand years) time scales. This is the case of the HFP sources J1511+0518 and OQ 208 where a relic from the past activity is found at about 50 pc from the reborn object (Orienti & Dallacasa 2008, Luo et al. 2007), indicating that, at least, in some objects the duty-cycle of the radio emission occurs on time-scale of  $10^3 - 10^4$  years.

Following the evolutionary path, CSO should evolve into FR II radio galaxies with ages of  $10^7 - 10^8$  years before the

radio emission enters in the relic phase. However, it is possible that not all the CSO would become FR II, and a population of fading short-lived objects under-represented in flux-limited catalogue is expected. If the interruption of the radio activity is a temporary phase and the radio emission from the central engine will restart soon, it is possible that the source will appear again as a CSO without the severe steepening at high frequencies. If this does not happen, the fate of the fading radio source is to emit at lower and lower frequencies, until it disappears at frequencies well below the MHz regime (Fig. 3).

## 5 Ambient medium

CSS and GPS radio sources are usually found in early-type gas-rich galaxies. The presence of significant amount of gas in young radio galaxies is supported by a larger incidence of HI absorption in these objects (Vermeulen et al. 2003, Pihlström, Conway, & Vermeulen 2003, Gupta et al. 2006) compared to what is typically found in old and larger radio sources (Morganti et al. 2001). This dense medium is likely the result of the merger that triggered the radio source (Morganti et al. 2004a). The knowledge of the distribution of the gas, either settled in a circumnuclear structure like a disk or a torus, or inhomogeneously distributed in clouds, provides important information on the environment in the innermost region of AGN and its role in the radio jet evolution.

Pihlström et al. (2003) found an empirical anti-correlation between the HI column density,  $N_{\text{HI}}$  and the source linear size in a sample of 41 CSS/GPS sources: smaller sources ( $<0.5$  kpc) have larger HI column densities than the larger sources ( $>0.5$  kpc). This result suggests that the HI gas is likely settled in a circumnuclear disk/torus with a radially declining density, and the absorption takes place only against the receding lobe. It is worth noting that the  $N_{\text{HI}}-LS$  anticorrelation does not seem to hold in the most compact HFP objects (Orienti, Morganti, & Dallacasa 2006), which highly deviate from the trend by Pihlström et al. (2003). The absence of high HI column density in very compact sources can be explained by both the orientation and the extreme compactness of the sources in a disk/torus scenario, in which our line of sight intersects the circumnuclear structure in its inner region where the low optical depth may be due to high spin and kinetic temperatures.

The presence of a gas distribution consistent with a circumnuclear disk/torus is supported by high-resolution VLBI observations that could trace either the atomic hydrogen across the source (e.g., 4C 31.04, Conway 1999; PKS 1946+708, Peak & Taylor 1999; B2352+495, Araya et al. 2010) or the ionized gas via free-free absorption (J1324+4048 and J0029+3457, Marr et al. 2014; J0111+3906, Marr, Taylor, & Crawford 2001), and by high-sensitivity observations of key molecular species such as CO, HCN, and  $\text{HCO}^+$  (e.g., 4C 31.04, Garcia-Burillo et al. 2009; OQ 208, Ocaña-Flaqueo et al. 2010).

Not all the ionized, atomic, and molecular gas is organized in a circumnuclear structure. As a consequence of the recent merger/accretion events experienced by the host galaxy, we expect the presence of unsettled, clumpy gas inhomogeneously distributed particularly in the innermost region. However, a secure prove of such clouds is difficult to obtain usually due to their low optical depth and small filling factor. However, if the cloud impacts with the jet temporarily confining its expansion. Shallow and broad HI absorption lines suggesting a jet-cloud interaction, were found in young or restarted objects, but the lack of angular resolution prevented a reliable interpretation of their origin, either circumnuclear or off-nuclear (Morganti, Tadhunter & Oosterloo 2005). An outstanding example is represented by the young, restarted GPS 4C 12.50, where VLBI observations locate the HI outflow of about  $10^4 M_{\odot}$  at about 100 pc from the nucleus where the radio jet interacts with the ISM, as well as around the associated radio lobe (Morganti et al. 2013). A possible molecular counterpart of the atomic outflow was found by Dasyra & Combes (2012) by deep CO observations. Interestingly, in the same source HI is observed in absorption also against the other lobe and may cause the bending of the jet (Morganti et al. 2004b). These results indicate that, despite the small filling factor of the clumpy medium, jet-cloud interaction can take place and may be responsible for some asymmetric radio sources observed. This may be the case of the two highly asymmetric CSS sources 3C 49 and 3C 268.3, in which HI absorption is observed only against the brightest lobe, which is also the closest to the core, although the non-detection in the other lobe might be due to sensitivity limitation (Labiano et al. 2006).

## 6 Asymmetries

As mentioned in Section 2, a large fraction of CSS/GPS sources have a very asymmetric structures (e.g., Saikia et al. 2003). A significant fraction ( $\sim 50\%$ ) of asymmetric sources have the brighter lobe that is also the closer to the core, which is opposite to what is expected if the source is not on the plane of the sky and some beaming effects and path delay are present. The brighter-when-closer trend suggests that the two jets are piercing their way through an inhomogeneous medium as pointed out by HI observations (see Section 5). The interaction between the advancing jet and a clumpy medium may enhance the luminosity due to high radiative losses which become predominant with respect to the adiabatic ones. Jet-cloud interactions should be more frequent during the first stages of the radio emission, when the jet is piercing its way through the dense and inhomogeneous gas of the host galaxy. Fig. 4 shows the flux density ratio versus the linear size of a sample of CSS/GPS and FR II (Orienti & Dallacasa 2008d). Sources larger than  $\sim 15$  kpc are more symmetric than the smaller ones.

The enhancement of the flux density may explain part of

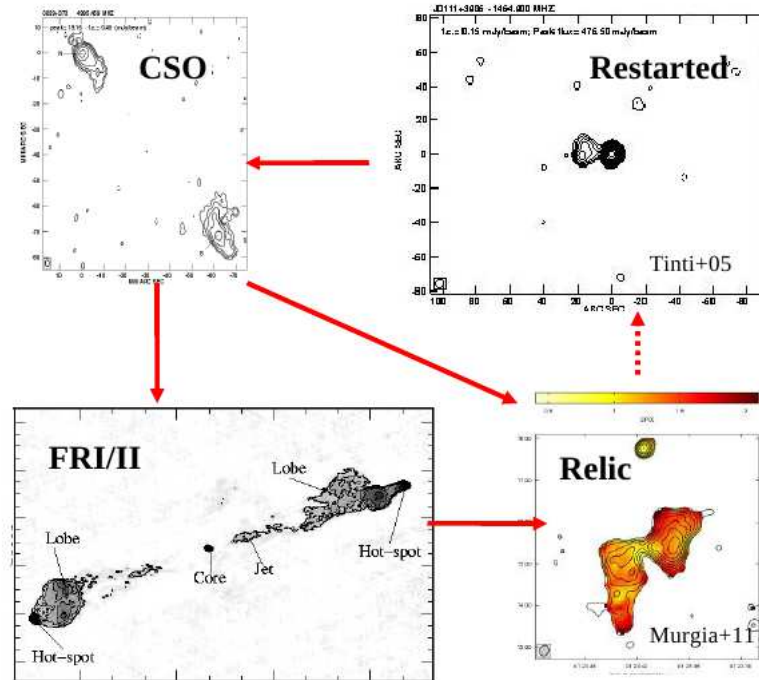


**Fig. 3** The evolutionary path of the radio emission. Young CSO (*top left*, image adapted from Orienti et al. 2004) may become either a classical large FR II (*bottom left*, image adapted from Mack et al. 2009) or a relic in the case of the activity phase switches off soon after its onset (*bottom right*, image adapted from Murgia et al. 2011). If the central engine goes through another active phase, a newly-born bright and compact object can be observed close to the relic of the previous activity (*top right*, image adapted from Tinti et al. 2005).

the high number counts of CSS/GPS objects in flux density limited samples. Furthermore, although the jet-medium interaction may not frustrate the source expansion for its whole lifetime, it may severely slow down its growth. The high fraction of CSS sources with a brighter-when-closer behaviour suggests that jet-cloud interactions are not so unlikely and it may cause an underestimate of the source age.

## 7 Concluding remarks

It has been more than two decades that compact steep spectrum and GHz-peaked spectrum radio sources are under investigation. During this time some questions got an answer, perhaps not unique, and new questions raised.

It is now fairly recognized that the majority of CSS and GPS radio sources, at least those optically associated with galaxy represent an early stage in the radio source evolution. These objects show two-sided structures similar to FR II radio galaxies, but on much smaller scales. No significant variability is observed. However, some level of variability explained in terms of adiabatic expansion in very young objects have been observed in a few radio sources.

The distinctive characteristic of CSS/GPS objects, i.e. the presence of a spectral turnover at low frequencies, is mainly

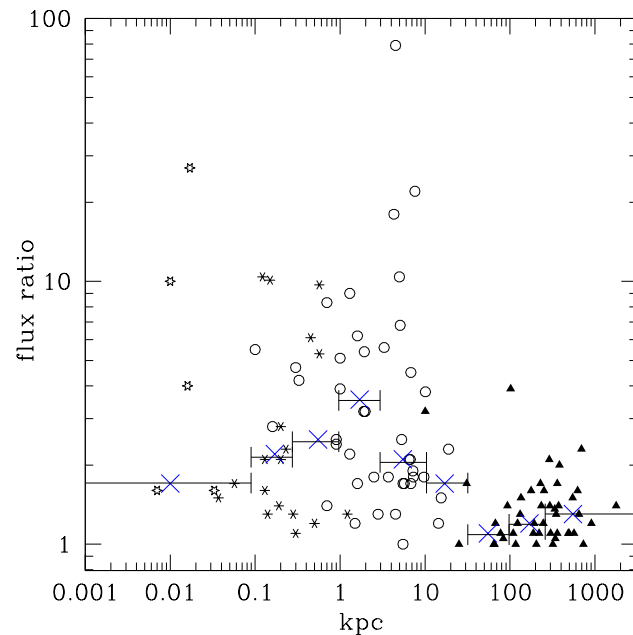


**Fig. 4** The flux density ratio of the lobes versus the source linear size. Crosses represent the median value computed on various range of linear sizes. Adapted from Orienti & Dallacasa (2008d).



due to SSA, although an additional contribution from FFA is detected in the most compact objects. The ambient medium enshrouding the radio emission is rich and inhomogeneous, favouring interactions between the jet and dense clouds. The high fraction of asymmetric sources, that is much higher than in extended FR II galaxies, points out how frequently a cloud can impact with one jet, temporarily confining, or at least slowing down, its advance speed, and enhancing the synchrotron emission. This may explain part of the excess in the number counts in flux limited sample. In fact, CSS/GPS are too many, even if we assume a decrease of the luminosity as they grow. This is predicted by the evolutionary models developed taking into account the ambient medium, and is confirmed by observations of samples of CSS/GPS spanning a large range of linear size.

Following the evolutionary scenario, GPS radio sources are the progenitors of CSS objects, which then should evolve in FR II radio galaxies. However, it seems that some CSS/GPS are short-lived objects, with ages up to  $10^3 - 10^4$  years, which may never become large sources with size of hundred of kpc or more. Only a handful of CSS/GPS have been recognized to be in a relic phase on the basis of the absence of active regions. These objects are under-represented in flux-limited catalogues due to the steepness of their synchrotron spectrum. The advent of the new radio facilities, like LOFAR, Merkaat, ASKAP, and SKA, will provide a step forward in estimating the incidence of short-lived and/or recurrent objects, providing a further piece in the puzzle of our understanding of the radio emission phenomenon.

*Acknowledgements.* I would like to thank Daniele Dallacasa for all the helpful and constructive discussions about the topics presented in this work.

## References

- Alexander, P.: 2000, MNRAS, 319, 8  
 Araya, E.D., Rodriguez, C., Pihlström, Y., et al.: 2010, AJ, 139, 17  
 Bicknell, G.V., Dopita, M.A., O’Dea, C.P.: 1997, ApJ, 485, 112  
 Brienza, M., et al.: 2015, AN, this issue  
 Brocksopp, C., Kaiser, C.R., Schoenmakers, A.P., de Bruyn, A.G.: 2007, MNRAS, 382, 1019  
 Burns, B.F.: 1966, MNRAS, 133, 6  
 Callingham, B.M., Gaensler, B.M., Ekers, R.D., et al.: 2015, ApJ, in press  
 Cassaro, P., Dallacasa, D., Stanghellini, C.: 2009, AN, 330, 203  
 Conway, J.E.: 1999, NewAR, 43, 509  
 Cotton, W.D., Dallacasa, D., Fanti, C., et al.: 2003, PASA, 20, 12  
 Cotton, W.D., Fanti, C., Fanti, R., Bicknell, G., Spencer, R.E.: 2006, A&A, 448, 535  
 Dallacasa, D., Stanghellini, C., Centonza, M., Fanti, R.: 2000, A&A, 363, 887  
 Dallacasa, D., Tinti, S., Fanti, C., et al.: 2002, A&A, 389, 115  
 Dallacasa, D., Orienti, M., Fanti, C., Fanti, R., Stanghellini, C.: 2014, MNRAS, 433, 147  
 Dallacasa, D., Orienti, M.: 2015, AN, this issue  
 Dasyra, K.M., Combes, F.: 2012, A&A, 541, 7  
 Fanaroff B.L., Riley J.M.: 1974, MNRAS, 167, 31  
 Fanti, R., Fanti, C., Schilizzi, R.T., et al.: 1990, A&A, 231, 333  
 Fanti, C., Fanti, R., Dallacasa, D., et al.: 1995, A&A, 302, 317  
 Fanti, C., Pozzi, F., Fanti, R., et al.: 2000, A&A, 358, 499  
 Fanti, C., Pozzi, F., Dallacasa, D., et al.: 2001, A&A, 369, 380  
 Fanti, C., Branchesi, M., Cotton, W.D., et al.: 2004, A&A, 427, 465  
 Fanti, C.: 2009, AN, 330, 120  
 Garcia-Burillo, S., Combes, F., Usero, A., Fuente, A.: 2009, AN, 330, 245  
 Giroletti, M., Polatidis, A.: 2009, AN, 330, 193  
 Gugliucci, N.E., Taylor, G.B., Peck, A.B., Giroletti, M.: 2005, ApJ, 622, 136  
 Gupta, N., Salter, C.J., Saikia, D.J., Ghosh, T., Jeyakumar, S.: 2006, MNRAS, 373, 972  
 Hancock, P.J., Sadler, E.M., Mahony, E.K., Ricci, R.: 2010, MNRAS, 408, 1187  
 Kellermann, K.I., Pauliny-Toth, I.I.K.: 1981, ARA&A, 19, 373  
 Kunert, M., Marecki, A., Spencer, R.E., Kus, A.J., Niezgodna, J.: 2002, A&A, 391, 47  
 Kunert-Bajraszewska, M., Marecki, A., Thomasson, P., Spencer R.E.: 2005, A&A, 440, 93  
 Kunert-Bajraszewska, M., Marecki A., Thomasson P.: 2006, A&A, 450, 945  
 Kunert-Bajraszewska, M., Gawronski, M.P., Labiano, A., Siemiginowska, A.: 2010, MNRAS, 408, 2261  
 Labiano, A., Vermeulen, R. C., Barthel, C. P., et al.: 2006, A&A, 447, 481  
 Luo, W.-F., Yang, J., Cui, L., Liu, X., Shen, Z.-Q.: 2007, ChJAA, 7, 611  
 Mack, K.-H., Prieto, M.A., Brunetti, G., Orienti, M.: 2009, MNRAS, 392, 705  
 Mantovani, F., Mack, K.-H., Montenegro-Montes, F.M., Rossetti, A., Kraus, A.: 2009, A&A, 502, 61  
 Mantovani, F., Bondi, M., Mack, K.-H.: 2011, A&A, 533, 79  
 Mantovani, F., Rossetti, A., Junor, W., Saikia, D.J., Salter, C.J.: 2013, A&A, 555, 4  
 Marr, J.M., Taylor, G.B., Crawford, F., III: 2001, ApJ, 550, 160  
 Marr, J.M., Perry, T.M., Read, J., Taylor, G.B., Morris, A.O.: 2014, ApJ, 780, 178  
 Mingaliyev, M.G., Sotnikova, Yu.V., Tornainen, I., Tornikoski, M., Udovitskiy, R.Yu.: 2012, A&A, 544, 25  
 Morganti, R., Oosterloo, T.A., Tadhunter, C.N., et al.: 2001, MNRAS, 323, 331  
 Morganti, R., Greenhill, L.J., Peck, A.B., Jones, D. L., Henkel, C.: 2004a, NewAR, 48, 1195  
 Morganti, R., Oosterloo, T., Tadhunter, C. N., et al.: 2004b, A&A, 424, 119  
 Morganti, R., Tadhunter, C.N., Oosterloo, T.A.: 2005, A&A, 444, 9  
 Morganti, R., Fogasy, J., Paragi, Z., Oosterloo, T., Orienti, M.: 2013, Science, 341, 1082  
 Murgia, M.: 2003, PASA, 20, 19  
 Murgia, M., Fanti, C., Fanti, R., et al.: 2009, A&A, 345, 769  
 Murgia, M., Parma, P., Mack, K.-H., et al.: 2011, A&A, 526, 148  
 Nagai, H., Inoue, M., Asada, K., Kameno, S., Doi, A.: 2006, ApJ, 648, 148  
 Ocaña-Flaquer, B., Leon, S., Combes, F., Lim, J.: 2010, A&A, 518, 9  
 O’Dea, C.P., Baum, S.A.: 1997, AJ, 113, 148  
 Orienti, M., Dallacasa, Tinti, S., Stanghellini, C.: 2006, A&A, 450, 959  
 Orienti, M., Dallacasa, D., Stanghellini, C.: 2007, A&A, 475, 813  
 Orienti, M., Dallacasa, D.: 2008a, A&A, 487, 885

- Orienti, M., Dallacasa, D.: 2008b, *A&A*, 477, 807  
Orienti, M., Dallacasa, D.: 2008c, *A&A*, 479, 409  
Orienti, M., Dallacasa, D.: 2008b, *ASPC*, 386, 196  
Orienti, M., Murgia, M., Dallacasa, D.: 2010, *MNRAS*, 402, 1892  
Orienti, M., Dallacasa, D., Stanghellini, C.: 2010, *MNRAS*, 408, 1075  
Orienti, M., Dallacasa, D.: 2012, *MNRAS*, 424, 532  
Pacholczyk, A.G.: 1970, *Radio Astrophysics* (San Francisco: Freeman & Co.)  
Parma P., Murgia M., de Ruiter H. R., Fanti R., Mack K.-H., Govoni F.: 2007, *A&A*, 470, 875  
Peck, A.B., Taylor, G.B., Conway, J.E.: 1998, *ApJ*, 521, 103  
Peck, A.B., Taylor, G.B.: 2000, *ApJ*, 534, 90  
Perucho, M.: 2015, *AN*, this issue  
Pihlström, Y.M., Conway, J.E., Vermeulen, R.C.: 2003, *A&A*, 404, 871  
Polatidis, A.G.: 2009, *AN*, 330, 149  
Polatidis, A.G., Conway, J.E.: 2003, *PASA*, 20, 69  
Readhead, A.C.S.: 1994, *ApJ*, 426, 51  
Rossetti, A., Mantovani, F., Dallacasa, D., Fanti, C., Fanti, R.: 2004, *A&A*, 434, 449  
Rossetti, A., Fanti, C., Fanti, R., Dallacasa, D., Stanghellini, C.: 2006, *A&A*, 449, 49  
Rossetti, A., Dallacasa, D., Fanti, C., Fanti, R., Mack, K.-H.: 2008, *A&A*, 487, 865  
Saikia, D.J., Gupta, N.: 2003, *A&A*, 405, 499  
Saikia, D.J., Jeyakumar, S., Mantovani, F., Salter, C.J., Spencer, R.E., Thomasson, P., Wiita, P.J.: 2003, *PASA*, 20, 50  
Scott, M.A., Readhead, A.C.S.: 1977, *MNRAS*, 180, 539  
Shulevski, A., Morganti, R., Oosterloo, T., Struve, C.: 2012, *A&A*, 545, 91  
Siemiginowska, A., Cheung, C.C., LaMassa, S., et al.: 2005, *ApJ*, 632, 110  
Snellen, I.A.G., Schilizzi, R.T., de Bruyn, A.G., et al.: 1998, *A&AS*, 131, 435  
Snellen, I.A.G., Schilizzi, R.T., Miley, G.K., et al.: 2000, *MNRAS*, 319, 445  
Snellen, I.A.G., Mack, K.-H., Schilizzi, R.T., Tschager, W.: 2004, *MNRAS*, 348, 227  
Spencer, R.E., McDowell, J.C., Charlesworth, M., et al.: 1989, *MNRAS*, 240, 657  
Stanghellini C., O'Dea, C.P., Dallacasa, D., et al.: 1998, *A&AS*, 131, 303  
Stanghellini, C., Dallacasa, D., Orienti, M.: 2009, *AN*, 330, 223  
Sutherland R.S., Bicknell G.V.: 2007, *ApJS*, 173, 37  
Tingay, S.J., de Kool, M.: 2003, *AJ*, 126, 723  
Tingay, S.J., Macquart, J.-P., Collier, J.D., et al.: 2015, *AJ*, 149, 74  
Tinti, S., Dallacasa, D., de Zotti, G., Celotti, A., Stanghellini, C.: 2005, *A&A*, 432, 31  
Tornainen, I., Tornikoski, M., Teräsranta, H., Aller, M.F., Aller, H.D.: 2005, *A&A*, 435, 839  
Tornainen, I., Tornikoski, M., Lähtenmäki, A., Aller, M.F., Aller, H.D., Mingaliev, M.G.: 2007, *A&A*, 469, 451  
Tremblay, S., Taylor, G.B., Helmboldt, J.F., Fassnacht, C.D., Roman, R.W.: 2009, *AN*, 330, 206  
Vermeulen, R.C., Pihlström, Y.M., Tschager, W., et al.: 2003, *A&A*, 404, 861  
Wilkinson, P.N., Polatidis, A.G., Readhead, A.C.S., Xu, W., Pearson, T.J.: 1994, *ApJ*, 432, 87